ChemPubSoc Europe

DOI: 10.1002/ejic.201501175

EurJIC European Journal of Inorganic Chemistry

Full Paper

CLUSTER ISSUE

Spin-Crossover Compounds

Solvent Influence on the Magnetic Properties of Iron(II) Spin-Crossover Coordination Compounds with 4,4′-Dipyridylethyne as Linker

Katja Dankhoff,[a] Charles Lochenie,[a] Florian Puchtler,[b] and Birgit Weber*[a]

Abstract: New iron(II) coordination polymers with solvent-dependent spin-crossover behaviour have been synthesised by using an N_2O_2 Schiff base like ligand and 4,4′-dipyridylethyne as the bridging axial ligand in different solvents. The effects of different solvents and preparation methods (temperature, concentration) on the magnetic properties have been investigated. Annealing the coordination polymers prepared by the same method but in different solvents led to the same compound exhibiting the same three-step spin crossover independent of the magnetic properties of the solvated species. The X-ray structures of the axial ligand, an iron(II) dimer and one of the iron(II) coordination polymers are discussed. Powder X-ray diffraction analysis was additionally used for further comparison of the compounds.

Introduction

The synthesis of functional coordination networks with switchable magnetic properties is a highly active area of research.[1,2] One possibility for realising such systems is the integration of spin-crossover (SCO) centres in coordination polymers or networks. Such materials are known for their ability to be switched between two different electronic states by a wide variety of physical and chemical stimuli.[3] This switching process is accompanied by a change in the physical properties of the material, for example, the magnetism or colour. The possibility of realising guest-dependent spin transitions in porous SCO materials[2,4,5] in combination with the read-out possibilities due to the associated changes makes this substance class highly interesting for applications in the field of sensing.[6]

The influence of solvent molecules included in the crystal packing on the SCO properties has already been documented for many different systems.[7] For the complexes investigated by our group, this is most commonly observed for coordination polymers, for which different solvents used in the synthesis often lead to different magnetic properties.[8–16] In contrast, such changes are rare for mononuclear complexes.[17] So far, however, the different magnetic properties have always been associated with differences in the packing of the polymer chains. As a consequence of this, an exchange of solvent molecules, as already realised, for example, for porous Hoffman clathrate systems, was not possible.[4,18,19]

In this work we present the synthesis of coordination polymers with bpey (4,4′-dipyridylethyne) as a rigid linker. On the one hand, rigid linkers are a pre-requisite for the observation of cooperative spin transitions.[20] Additionally, this linker is longer than 4,4′-bipyridine, already used as a rigid linker for the formation of coordination polymers of the complexes investigated by our group. Thus, the formation of porous structures for the inclusion of solvent molecules is more likely and due to the rigid structure, the chances of reversibility are higher. Indeed, Hofmann clathrate complexes with bpey as ligand showing different magnetic behaviours depending on the amount of solvent have also been reported.[18,19]

Results and Discussion

Synthesis

The ligand bpey was synthesised as reported by Tanner and Ludi[21] by bromination of *trans*-4,4′-dipyridylethylene (bpee) and elimination of two molecules of HBr from 1,2-dibromo-1,2-pyridylethane by using *t*BuONa in *t*BuOH. The purity of the product was confirmed by elemental analysis, ^{1}H NMR spectroscopy, mass spectrometry and IR spectroscopy. The general synthesis for the iron(II) complexes is based on a ligand-exchange reaction between the axial methanol ligands of the already reported iron(II) precursor[22] complex and the axial ligand bpey (Scheme 1). Three different methods were used for the synthesis of the iron(II) complexes.

Method 1: The aim of method 1 was to precipitate the compound in boiling solvent. Therefore a concentrated solution of

---

[a] *Lehrstuhl für Anorganische Chemie II, Universität Bayreuth, Universitätsstraße 30, NW 1, 95440 Bayreuth, Germany*
E-mail: weber@uni-bayreuth.de
http://www.ac2-weber.uni-bayreuth.de

[b] *Lehrstuhl für Anorganische Chemie I, Universität Bayreuth, Universitätsstraße 30, NW 1, 95440 Bayreuth, Germany*
http://www.ac1.uni-bayreuth.de

Supporting information and ORCID(s) from the author(s) for this article are available on the WWW under http://dx.doi.org/10.1002/ejic.201501175.

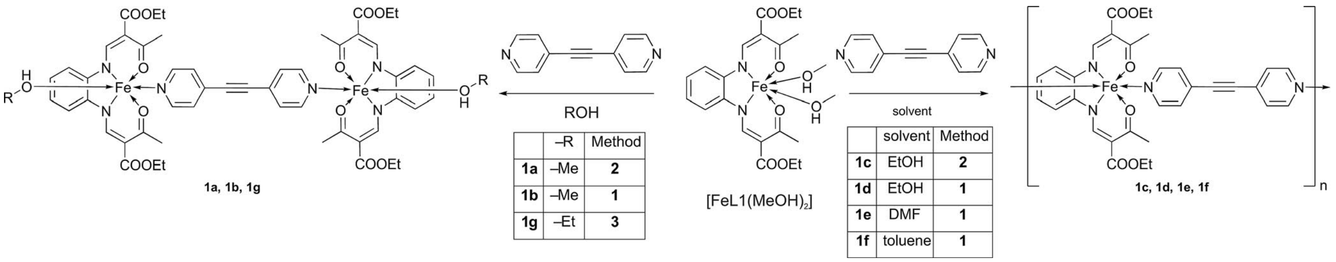

	–R	Method
1a	–Me	2
1b	–Me	1
1g	–Et	3

	solvent	Method
1c	EtOH	2
1d	EtOH	1
1e	DMF	1
1f	toluene	1

Scheme 1. Synthesis of the iron(II) complexes discussed in this work.

the precursor complex (0.2 g in 15 mL of solvent) and 2 equivalents of the ligand bpey were heated at reflux for 1 hour and the precipitate was filtered off.

Method 2: The aim of method 2 was to precipitate the compound at room temperature. Therefore a diluted solution of the precursor complex (0.2 g in 60 mL of solvent) and 2 equivalents of the ligand were heated at reflux and cooled to room temperature. A precipitate was obtained after several days and filtered off.

Method 3: The aim of method 3 was to obtain crystals suitable for X-ray structure analysis. Therefore a slow diffusion setup was prepared for a solution of the precursor complex and a solution of the ligand.

Methods 1 and 2 were used to investigate whether the temperature of precipitation has an influence on the magnetic properties. This could be the case if the complex precipitates either in the high- or low-spin state and has already been observed for other SCO complexes of this ligand type.[8,14] Scheme 1 displays the general pathway for the synthesis of the iron(II) complexes. The complexes all precipitated as very dark, microcrystalline materials with varying solvent contents according to elemental analysis, mass spectrometry, thermogravimetric analysis (TGA; see Figure S1 in the Supporting Information), and IR spectroscopy. Table 1 gives an overview of all the iron(II) complexes prepared, the corresponding solvent used in the synthesis and the included solvent content. Coordination polymers were obtained in most cases, as expected for this type of compound.[10] However, in three cases dimers were obtained with this axial ligand; atomic absorption spectroscopy was used to determine the percentage of iron(II) and distinguish between polymers and dimers for all the high-spin (HS) complexes. Dimers have not yet been reported for this class of iron(II) compound with phenylenediamine-based ligands. However, for modified ligands based on 3,4-alkoxy-substituted phenylenediamine, such pentacoordinate or hexacoordinate structures are frequently observed.[23]

Table 1. Iron(II) complexes with the solvents and methods used for their synthesis.

	Complex	Solvent	Method
1a	μ-(bpey)-$[FeL1(MeOH)]_2$	MeOH	2
1b	μ-(bpey)-$[FeL1(MeOH)]_2$	MeOH	1
1c	$\{[FeL1(bpey)]\cdot 0.5EtOH\}_n$	EtOH	2
1d	$[FeL1(bpey)]_n$	EtOH	1
1e	$\{[FeL1(bpey)]\cdot dmf\}_n$	dmf	1
1f	$\{[FeL1(bpey)]\cdot 1.25toluene\}_n$	toluene	1
1g	μ-(bpey)-$[FeL1(EtOH)]_2$	EtOH	3

Crystal Structure Analysis

Crystals suitable for X-ray structure analysis were obtained for the ligand bpey by recrystallisation of the ligand from petroleum ether. Even though the synthesis of the ligand bpey has been reported, to the best of our knowledge, its X-ray structure was not available until now. The crystal data were collected at 133 K and are presented in Table S1 in the Supporting Information. An ORTEP drawing of the ligand is shown in Figure 1. The ligand bpey crystallises in the monoclinic space group *C2/m*. The asymmetric unit contains one quarter of the molecule. The bond lengths and angles are given in Table 2. The triple bond is linear with a >C–C≡C angle of 180° and the pyridyl rings are coplanar.

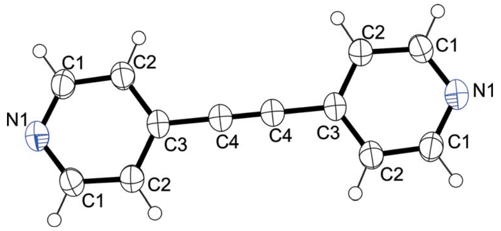

Figure 1. ORTEP drawing of bpey. Ellipsoids are drawn at the 50 % probability level.

Table 2. Bond lengths and angles of bpey.

Bond length [Å]		Bond angle [°]	
N1–C1	1.3348(17)	N1–C1–C2	124.14(13)
C1–C2	1.384(2)	C1–C2–C3	118.77(13)
C2–C3	1.3868(7)	C2–C3–C2	117.92(15)
C3–C4	1.439(3)	C3–C4–C4	180.00(19)
C4–C4	1.199(3)	C2–C3–C3–C2	0.07

Crystals suitable for X-ray structure analysis of the dimer **1g** were obtained by slow diffusion of the iron(II) precursor and bpey in EtOH at room temperature. The crystal data were collected at 133 K and are presented in Table S1 in the Supporting Information. An ORTEP drawing of the complex is shown in

Figure 2. The compound crystallises in the triclinic space group $P\bar{1}$. The asymmetric unit contains one and a half molecules of the dimer. Selected bond lengths and angles are given in Table 3. The sixth coordination site of the iron centre is occupied by an ethanol molecule, the methyl group of which is disordered over more than two positions (probably rotating). This disorder could not be solved.

1g

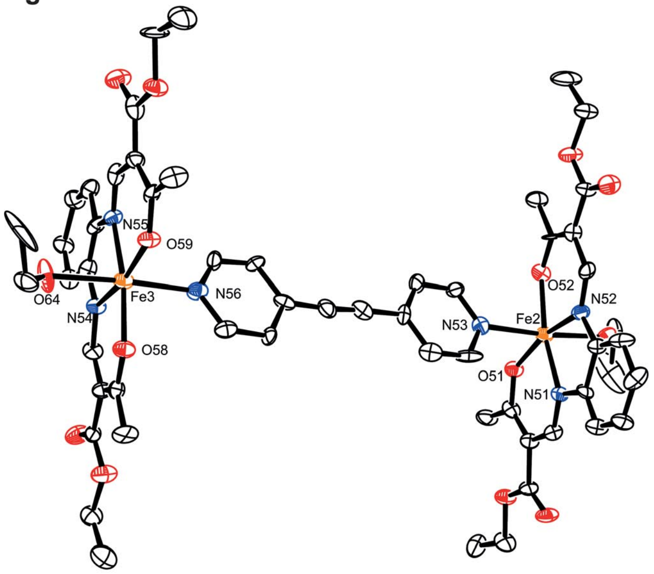

1e

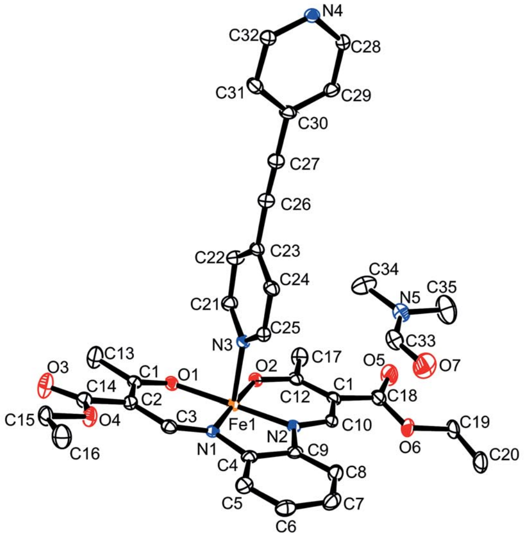

Figure 2. ORTEP drawings of **1g** (top) and **1e** (bottom). Hydrogen atoms have been omitted for clarity. Ellipsoids are drawn at the 50 % probability level.

The iron(II) centres of **1g** have an octahedral N_3O_3 coordination sphere, with the ligand bpey linking the two iron(II) centres. The average bond lengths are 2.08 (Fe–N_{eq}), 2.00 (Fe–O_{eq}), 2.26 (Fe–N_{ax}) and 2.24 Å (Fe–O_{ax}). The average O_{eq}–Fe–O_{eq} angle of 108° is clearly in the range typical of the HS state for iron(II) complexes of this type.[17,24] The average L_{ax}–Fe–L_{ax} angle of 175.1° does not differ significantly from the expected angle of 180° for an ideal octahedron. The >C–C≡C angle has an average value of 176.7°, which indicates a slight bending of the ligand. The torsion angle between the pyridyl rings of the ligand bpey is small with an average value of 1.2°. The OH groups of the coordinating ethanol molecules in the asymmetric unit are donors for hydrogen bonds with a carbonyl oxygen of a neighbouring molecule (O17–H17A···O60, O57–H57A···O55 and O64–H64···O15). Through these hydrogen bonds, the dimers form zig-zag chains along the vector [1–11]. The details of the hydrogen bonds are summarised in Table 4 and the molecular packing of the compound in the crystal is shown in Figure 3.

Table 4. Overview of the intermolecular hydrogen bonds in **1g** and **1e**.

	D–H···A	D–H [Å]	H···A [Å]	D···A [Å]	D–H···A [°]
1g	O17–H17A···O60^a	0.84	2.01	2.729(12)	143
	O57–H57A···O55^b	0.84	1.97	2.748(12)	154
	O64–H64···O15^a	0.84	1.92	2.714(11)	158
1e	C24–H24···O7^c	0.95	2.38	3.010(3)	122
	C25–H25···O7^c	0.95	2.43	3.039(3)	122

a: 2 – *x*, 1 – *y*, 2 – *z*, b: 1 – *x*, 1 – *y*, 1 – *z*, c: 2 – *x*, –*y*, 2 – *z*

Crystals of the coordination polymer **1e** were obtained directly from the synthesis. The crystal data were collected at 133 K and are presented in Table S1 in the Supporting Information. An ORTEP drawing of the asymmetric unit is given in Figure 2. The coordination polymer crystallises in the monoclinic space group $P2_1/c$. The asymmetric unit contains the monomeric unit of the coordination polymer $[FeL1(bpey)]_n$ and one non-coordinating dmf molecule. Selected bond lengths and angles are given in Table 3. The iron(II) centre has an octahedral N_4O_2 coordination sphere. The average bond lengths are 1.90 (Fe–N_{eq}), 1.94 (Fe–O_{eq}) and 1.99 (Fe–N_{ax}). The O_{eq}–Fe–O_{eq} angle

Table 3. Spin state, selected bond lengths and angles within the inner coordination sphere of the iron(II) complexes discussed in this work, and angles and torsion angles of the triple bond of bpey.[a]

	S	Fe–N_{eq} [Å]	Fe–O_{eq} [Å]	Fe–N_{ax} [Å]	Fe–O_{ax} [Å]	O_{eq}–Fe–O_{eq} [°]	L_{ax}–Fe–L_{ax} [°]	bpey >C–C≡C [°]	Torsion bpey [°]
1g	2	2.071(10)	2.007(8)	2.275(9)	2.225(8)	107.7(3)	174.7(3)	178.3(12)	0.48
		2.081(10)	1.989(8)	2.258(9)	2.247(8)	107.4(3)	175.0(3)	177.1(14)	1.60
		2.075(10)	2.015(8)	2.250(9)	2.236(8)	107.3(3)	175.5(3)	174.7(14)	1.45
		2.070(10)	1.994(8)						
		2.095(9)	1.988(8)						
		2.086(10)	2.012(8)						
1e	0	1.9004(17)	1.9427(14)	1.9865(15)		89.49(6)	175.54(7)	179.3(2)	88.76
		1.9052(17)	1.9472(13)	1.9833(15)				176.4(2)	88.52

[a] Crystal data determined at 133 K.

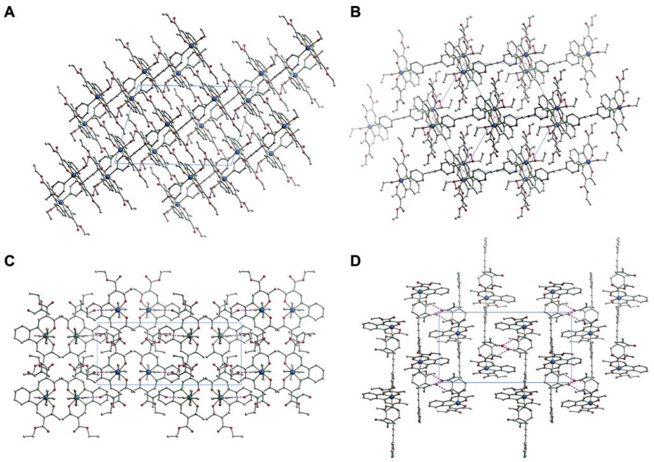

Figure 3. Molecular packing of compounds **1g** (top: A: along [010]; B: along [111]) and **1e** (bottom: C: along [001]; D: along [100]) in the crystal. Hydrogen atoms not involved in hydrogen bonds have been omitted for clarity. Hydrogen bonds are drawn as dashed lines.

is 89.49(6)°, clearly in the range for LS iron(II).[17,24] This is in agreement with the results of the magnetic measurements, which show that the full HS state is only reached above room temperature, therefore it was not possible to determine the structure of the HS state. The L_{ax}–Fe–L_{ax} angle of 175.54(7)° does not differ significantly from the expected angle of 180° for a perfect octahedron. The bidentate ligand bpey links the iron(II) centres in infinite chains along [001]. The average >C–C≡C angle of 177.85° indicates a slight bending of the ligand. The two pyridyl rings of bpey are almost perpendicular to each other with an average torsion angle of 88.64°. In addition to the monomeric unit of the complex, the asymmetric unit contains one molecule of dmf connected through hydrogen bonds to one pyridyl ring of the axial ligand. Details of the hydrogen bonds are given in Table 4; two aromatic CH groups of the axial ligand bpey (C24–H24 and C25–H25) are the donor groups and the carbonyl oxygen (O7) of the dmf is the acceptor group. These hydrogen bonds are the reason for the bending of the axial ligand. The packing of the molecules in the crystal with the hydrogen bonds is shown in Figure 3.

Magnetism

Magnetic susceptibility measurements were performed at an applied field of 5000 G by using a SQUID magnetometer over a range of temperatures to follow the spin transition (ST).

All the coordination polymers **1c**–**f** show solvent-dependent SCO behaviour. The $\chi_M T$ products for the dimeric complexes **1a**, **1b** and **1g** are in the range expected for dimeric HS iron(II) complexes ($S_1 = S_2 = 2$; expected spin-only value: $\chi_M T = 6\ \mathrm{cm^3\,K\,mol^{-1}}$) with a significant orbital momentum contribution. The room temperature values are 7.56 (**1a**), 7.16 (**1b**) and 7.60 $\mathrm{cm^3\,K\,mol^{-1}}$ (**1g**). The plots of $\chi_M T$ versus T in the ranges 300–50 K (**1a** and **1g**) and 300–4 K (**1b**) for these complexes are presented in Figure S2 in the Supporting Information. In all cases, the $\chi_M T$ product does not change significantly with temperature, which indicates the absence of any strong ex-

Table 5. Overview of the magnetic properties, $T_{1/2}$ values, values of the $\chi_M T$ product at the corresponding temperatures, and HS residues of the synthesised compounds.

	SCO	$T_{1/2}$ [K]	$\chi_M T$ (HS) [$\mathrm{cm^3\,K\,mol^{-1}}$]	$\chi_M T$ (LS) [$\mathrm{cm^3\,K\,mol^{-1}}$]	γ_{HS}
1a	HS	–	7.56 (300 K)	–	1
1b	HS	–	7.16 (300 K)	–	1
1c	stepwise, abrupt with hysteresis	↓ 170 ↑ 190	3.37 (300 K)		1 (300 K)
		↓ 110 ↑ 135	1.87 (145 K)		0.55 (145 K)
				0.43 (50 K)	0.13 (50 K)
	incomplete, abrupt with hysteresis[a]	↓ 175 ↑ 185	3.37 (300 K)		1 (300 K)
			1.63 (160 K)		0.48 (160 K)
				0.85 (50 K)	0.25 (50 K)
1d	multi-step, gradual, abrupt	320	3.34 (400 K)		1 (400 K)
		210	1.92 (250 K)		0.57 (250 K)
		140	1.12 (175 K)		0.34 (175 K)
				0.18 (50 K)	0.05 (50 K)
	multi-step, gradual, abrupt[a]	320	3.34 (400 K)		1 (400 K)
		210	1.77 (250 K)		0.53 (250 K)
		140	0.96 (175 K)		0.29 (175 K)
				0.12 (50 K)	0.04 (50 K)
1e	gradual	305	3.65 (400 K)		1 (400 K)
				0.06 (200 K)	0.02 (200 K)
	multi-step, gradual, abrupt[a]	320	3.65 (400 K)		1 (400 K)
		210	2.05 (250 K)		0.56 (250 K)
		140	1.20 (175 K)		0.33 (175 K)
				0.38 (50 K)	0.10 (50 K)
1f	gradual	125	2.99 (200 K)		1 (200 K)
				1.39 (50 K)	0.46 (50 K)
	multi-step, gradual, abrupt[a]	320	3.22 (400 K)		1 (400 K)
		210	1.74 (250 K)		0.54 (250 K)
		140	0.97 (175 K)		0.30 (175 K)
				0.19 (50 K)	0.06 (50 K)

[a] After annealing.

change interactions through the bpey ligand; the linker bpey is probably too long to allow an effective super-exchange pathway between the iron(II) centres. All measurements for the coordination polymers were taken in settle mode, but to show that there is no significant dependence on scan rate, the plots of $\chi_M T$ versus T for the sweep measurements of all complexes are presented in Figure S2 in the Supporting Information, as it has been shown that the scan rate can significantly influence the width of the hysteresis.[25] An overview of all the $\chi_M T$ values, the fraction of the HS state, and the SCO behaviour is presented in Table 5. The plots of $\chi_M T$ versus T in the temperature ranges of interest for the ST of complexes **1c**–**1f** are displayed in Figure 4. Plots of $\chi_M T$ versus T in the full temperature range of 50–400 K can be found in Figure S2 in the Supporting Information. Complex **1c** exhibits almost complete solvent-dependent SCO behaviour. The first cooling and heating cycle reveals a stepwise ST with hysteresis. The first step has a hysteresis width of 20 K with $T_1\downarrow$ = 170 K and $T_1\uparrow$ = 190 K. The second step has a hysteresis width of 25 K with $T_2\downarrow$ = 110 K and $T_2\uparrow$ = 135 K, and the complex is almost totally LS at 85 K. The $\chi_M T$ product is 3.37 cm^3 K mol^{-1} at 300 K and is typical of HS iron(II). It decreases to 1.87 cm^3 K mol^{-1} at 145 K (plateau), and after the second step it reaches 0.43 cm^3 K mol^{-1} at 50 K.

After heating the sample to 400 K and keeping it at this temperature for 1 hour to remove the included solvent molecules, the SCO behaviour changed. Now an incomplete spin transition with hysteresis is observed. The first step is similar to the first cooling and heating cycle with a hysteresis width of 10 K ($T_1\downarrow$ = 175 K and $T_1\uparrow$ = 185 K). After the first step the $\chi_M T$ value is 1.63 cm^3 K mol^{-1} at 160 K. On further cooling it gradually decreases until it reaches 0.85 cm^3 K mol^{-1} at 50 K. To rule out different iron sites (e.g., due to short polymer chains with EtOH coordination at the chain ends) as a reason for the remaining HS fraction, a Mössbauer spectrum was recorded at room temperature (see Figure S3 and Table S2 in the Supporting Information), which shows only one HS iron(II) site. Thus, other reasons are responsible for the incomplete spin transition.

Complex **1d** shows a multi-step ST over the complete temperature range studied (50–400 K). The first, rather gradual step takes place at 320 K with a third of the iron(II) centres undergoing the ST. The value of the $\chi_M T$ product decreases from 3.34 cm^3 K mol^{-1} at 400 K to 1.92 cm^3 K mol^{-1} at 250 K. The second, more abrupt step takes place at 210 K. Another third of the iron(II) centres undergo the ST with a value of the $\chi_M T$ product of 1.12 cm^3 K mol^{-1} at 175 K. The last, abrupt step in the transition takes place at 140 K. The remaining iron(II) cen-

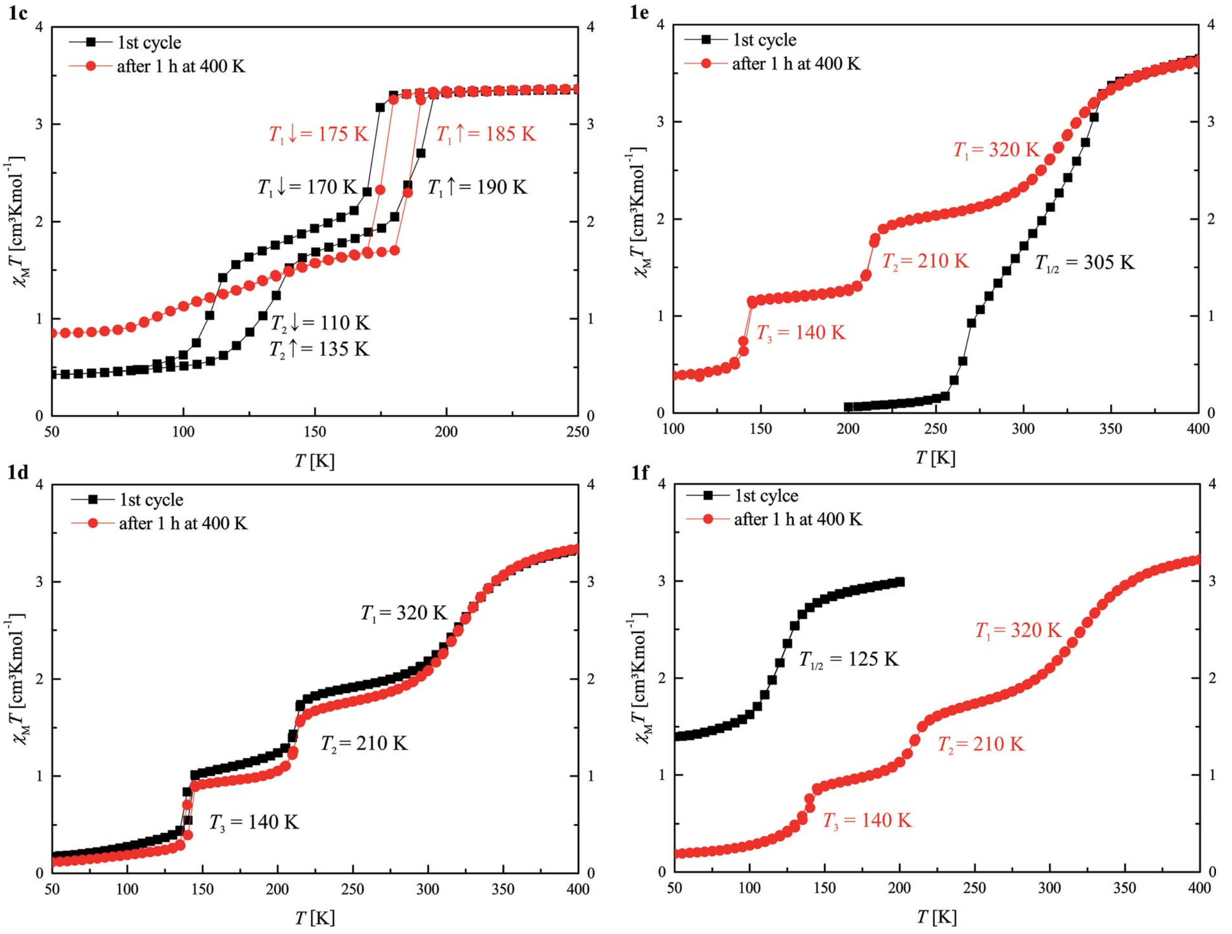

Figure 4. Plots of the $\chi_M T$ products versus T for compounds **1c** (left, top), **1d** (left, bottom), **1e** (right, top) and **1f** (right, bottom). Black squares represent the first cooling and heating cycle, red circles represent the cooling and heating cycle after annealing.

tres change their spin state to LS. The final $\chi_M T$ product is 0.18 cm^3 K mol^{-1} at 50 K. After heating to 400 K for 1 hour the SCO properties do not change significantly, the only change that can be observed is a small decrease in the value of the $\chi_M T$ product after each step in the ST (see Table 5).

Complexes **1e** and **1f** show a gradual, complete (**1e**) or incomplete (**1f**) ST with $T_{1/2}$ = 305 K for **1e** and $T_{1/2}$ = 125 K for **1f**. The value of the $\chi_M T$ product of **1e** is 0.06 cm^3 K mol^{-1} at 200 K, and therefore clearly in the range for LS iron(II). After the ST it has a value of 3.65 cm^3 K mol^{-1} at 400 K, which is typical for HS iron(II). Complex **1f** has a $\chi_M T$ product value of 2.99 cm^3 K mol^{-1} at 200 K and after the ST the value of the $\chi_M T$ product is 1.39 cm^3 K mol^{-1} at 50 K. After heating at 400 K for 1 hour, both complexes show the same ST as complex **1d** with just small differences in the values of the $\chi_M T$ product, which indicates that these complexes have the same "dry" phase.

Powder Diffraction Analysis

All the samples were subjected to powder X-ray diffraction analysis at relevant temperatures for the magnetic properties of the complexes. Two regions of the powder diffraction patterns are of special interest: the iron(II)–iron(II) distance is often observed between 7 and 10° and the inter-chain distance can be observed between 24 and 27°. These regions were determined by using Bragg's law ($\sin\theta = \lambda/2d$) and the results obtained for similar 1D chain compounds have already demonstrated that even changes in the Fe–Fe distances in the chain due to the spin transition can be explained (larger $\theta \rightarrow$ smaller d and vice versa).[15] The strong diffraction peaks in the region between 7 and 10° most likely arise from iron centres with a high electron density. Additionally, for most of the 1D coordination polymers synthesised by our group, the polymer chains are parallel, supporting a diffraction pattern dominated by inter-chain iron–iron distances. The powder X-ray diffraction patterns of the dimeric complexes **1a** and **1g** are similar and are shown in Figure S4 in the Supporting Information. The recorded and calculated spectra of the complexes **1c**–**1f** are shown in Figure 5. The spectra of each of **1c** and **1f** are the same at all the temperatures measured; the small shifts are due to the different temperatures at which the spectra were recorded. The powder diffraction spectra of **1d** at three different temperatures (100, 175 K and room temp.) look very similar. The disappearance of the peak at 8.46° (100 and 175 K) and the appearance of the peak at 8.35° (175 K and room temp., denoted by * in Figure 5) can be correlated to the change in the spin state of the iron(II) centre from LS (100 K) to almost HS (room temp.). The powder diffraction spectra of **1e** are drastically different at the two measured temperatures (calculated at 133 K, and measured at room temp.). For the complexes **1d**–**f**, a change in the position of the peak representative of the iron–iron distance can be observed depending on the temperature of the measurement. This change can be explained by the change in the spin state of the iron(II) centre. In the HS state, the peak has a position at a smaller 2θ angle (larger distance) than in the LS state. This is due to a volume change upon ST. Based on this data, a new structural phase corresponding to the plateau in the magnetic data cannot be ruled out. To further compare compounds **1d**–**f**, the powder patterns of **1e** and **1f** were recorded at room temperature after annealing. It can be seen that all the complexes are isostructural.

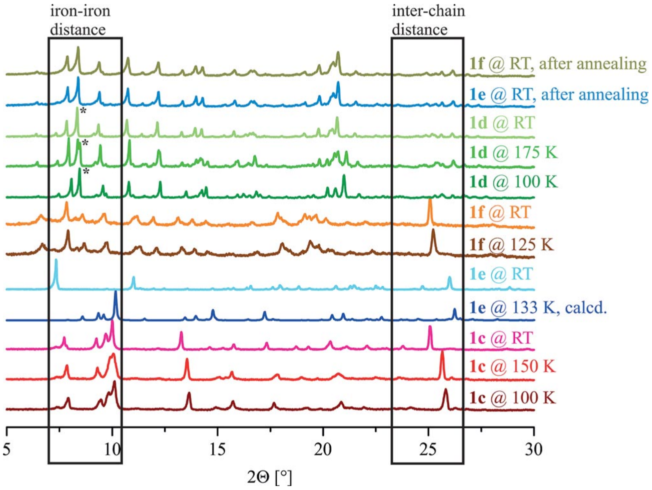

Figure 5. Powder X-ray diffraction patterns of **1c**–**f**.

Discussion

Of the seven synthesised complexes, three are dimers (**1a**, **1b** and **1g**) and therefore are HS over the complete temperature range studied. The remaining four synthesised coordination polymers show different SCO behaviour when solvated, also the powder X-ray diffraction patterns are different for these complexes. Once dried, the three complexes synthesised by the same method (for **1d**–**f**) but in different solvents show the same three-step ST, which indicates that annealing leads to a similar "dry phase". This can be seen in the powder X-ray diffraction patterns of the annealed complexes, which are all the same. The complexes have a different structure when solvated. Therefore the exchange of solvents is not possible. The complex synthesised by a different method (for **1c**) shows a different ST to the others, and also a different powder X-ray diffraction pattern. This indicates that the temperature of precipitation has a strong influence on the magnetic properties. The greater amount of solvent used in the synthesis caused a slower precipitation of the complex and therefore a different packing in the crystal. The solvent dependence of SCO behaviour has already been described for this type of compound but with *N*-(4-pyridyl)isonicotinamide as the axial ligand. In contrast to this linker, which has an amide group that can easily form hydrogen bonds with solvent molecules or neighbouring complexes,[15] bpey is a ligand that has no strong hydrogen-bond donor or acceptor atoms. Similar complexes with 4,4′-bipyridine as axial ligand show hysteretic SCO behaviour, but have no solvent included in the crystal packing.[14,26] As the ligand bpey is longer it leads to more space between the iron(II) centres and therefore there is a higher possibility that it will trap solvent molecules. The trapped solvent molecules form hydrogen bonds with the ligand bpey, as shown in the structure of **1e**, and significantly influence the SCO properties of the material. However, as only

1D coordination polymers are formed, the pores in the structure are not stable enough to allow the reversible binding of the solvent molecules.

Conclusions

In this report we have described the influence of solvent on the SCO properties of an iron(II) coordination polymer with a Schiff base like equatorial ligand and 4,4′-dipyridylethyne (bpey) as axial ligand. As has been shown previously,[8–16] the solvent has a significant influence on the SCO behaviour of this type of compound. Depending on the solvent used and preparation method, different iron(II) complexes were obtained. The first iron(II) dimers of this type of compound were obtained, and are HS over the complete temperature range studied (50–400 K). The iron(II) coordination polymers all exhibit SCO behaviour. For those synthesised by the same method but in different solvents, different spin transitions can be observed when solvated. Once fully dried, the complexes show the same, three-step spin transition over almost the entire temperature range studied (50–400 K). The powder X-ray diffraction patterns of the solvated complexes are different for each complex, but the same when fully dried. The iron(II) coordination polymer synthesised by a different method shows incomplete, but hysteretic SCO behaviour. The synthesis and characterisation of other complexes with bpey as axial ligand are currently ongoing, for example, with alkoxy derivatives of our Schiff base like ligands.[27]

Experimental Section

Materials and Methods: All syntheses involving iron(II) were carried out under argon using Schlenk tube techniques. The solvents used were of analytical grade and degassed with argon. The precursor complex [FeL1(MeOH)$_2$][22] and the axial ligand 4,4′-dipyridylethyne[21] were synthesized according to literature procedures. CHN analyses were performed with a Vario El III instrument from Elementar AnalysenSysteme. Mass spectra were recorded with a Finnigan MAT 8500 spectrometer with a MASPEC II data system.

μ-(bpey)-[FeL1(MeOH)]$_2$ (1a): A dark red-brown solution of [FeL1(MeOH)$_2$] (0.2 g, 0.395 mmol) and bpey (0.14 g, 0.777 mmol) in methanol (60 mL) was heated at reflux for 1 h. After cooling and leaving to stand at room temperature for 1 d, the black precipitate was filtered off, washed twice with methanol (3 mL) and dried in vacuo to give **1a**, yield 0.16 g (36 %). IR (neat): $\tilde{\nu}$ = 1686 (CO, s), 1564 (CO, s) cm^{-1}. MS (EI, +): *m/z* (%) = 442 (66) [$C_{20}H_{22}FeN_2O_6$]$^+$, 180 (100) [$C_{12}H_8N_2$]$^+$. $C_{54}H_{60}Fe_2N_6O_{14}$ (1128.78): calcd. C 57.46, H 5.36, N 7.45, Fe 9.89; found C 57.55, H 5.33, N 7.51, Fe 10.22.

μ-(bpey)-[FeL1(MeOH)]$_2$ (1b): A dark red-brown solution of [FeL1(MeOH)$_2$] (0.2 g, 0.315 mmol) and bpey (0.14 g, 0.777 mmol) in methanol (15 mL) was heated at reflux for 1 h. After cooling and leaving to stand at room temperature for 1 d, the black precipitate was filtered off, washed with methanol (5 mL) and dried in vacuo to give **1b**, yield 0.17 g (38 %). IR: $\tilde{\nu}$ = 1686 (CO, s), 1564 (CO, s) cm^{-1}. MS (EI, +): *m/z* (%) = 442 (66) [$C_{20}H_{22}FeN_2O_6$]$^+$, 180 (100) [$C_{12}H_8N_2$]$^+$. $C_{54}H_{60}Fe_2N_6O_{14}$ (1128.78): calcd. C 57.46, H 5.36, N 7.45, Fe 9.89; found C 57.27, H 5.36, N 7.44, Fe 10.89.

{[FeL1(bpey)]·0.5 EtOH}$_n$ (1c): A dark red-brown solution of [FeL1(MeOH)$_2$] (0.2 g, 0.315 mmol) and bpey (0.14 g, 0.777 mmol) in ethanol (60 mL) was heated at reflux for 1 h. After cooling and leaving to stand at room temperature for 1 d, the black precipitate was filtered off, washed twice with ethanol (3 mL) and dried in vacuo to give **1c**, yield 0.16 g (63 %). IR: $\tilde{\nu}$ = 1683 (CO, s), 1567 (CO, s) cm^{-1}. MS (EI, +): *m/z* (%) = 442 (66) [$C_{20}H_{22}FeN_2O_6$]$^+$, 180 (100) [$C_{12}H_8N_2$]$^+$. $C_{32}H_{30}FeN_4O_6$·0.5EtOH (645.49): calcd. C 61.40, H 5.15, N 8.68; found C 61.20, H 5.15, N 8.82.

[FeL1(bpey)]$_n$ (1d): A dark red-brown solution of [FeL1(MeOH)$_2$] (0.2 g, 0.315 mmol) and bpey (0.14 g, 0.777 mmol) in ethanol (15 mL) was heated at reflux for 1 h. After cooling to room temperature, the black precipitate was filtered off, washed twice with ethanol (5 mL) and dried in vacuo to give **1d**, yield 0.17 g (64 %). IR: $\tilde{\nu}$ = 1685 (CO, s), 1559 (CO, s) cm^{-1}. MS (EI, +): *m/z* (%) = 442 (66) [$C_{20}H_{22}FeN_2O_6$]$^+$, 180 (100) [$C_{12}H_8N_2$]$^+$. $C_{32}H_{30}FeN_4O_6$ (622.46): calcd. C 61.75, H 4.86, N 9.00; found C 61.32, H 5.12, N 8.93.

{[FeL1(bpey)]·dmf}$_n$ (1e): A dark red-brown solution of [FeL1(MeOH)$_2$] (0.2 g, 0.315 mmol) and bpey (0.14 g, 0.777 mmol) in dmf (15 mL) was heated at reflux for 20 min. After cooling and leaving to stand at room temperature for 5 d, the black crystals were filtered off and dried in vacuo to give **1e**, yield 0.1 g (46 %). IR: $\tilde{\nu}$ = 1676 (CO, s), 1561 (CO, s) cm^{-1}. MS (EI, +): *m/z* (%) = 442 (66) [$C_{20}H_{22}FeN_2O_6$]$^+$, 180 (100) [$C_{12}H_8N_2$]$^+$. $C_{32}H_{30}FeN_4O_6$·dmf (695.55): calcd. C 60.44, H 5.36, N 10.07; found C 60.35, H 5.37, N 10.03.

{[FeL1(bpey)]·1.25toluene}$_n$ (1f): A dark red-brown solution of [FeL1(MeOH)$_2$] (0.2 g, 0.315 mmol) and bpey (0.14 g, 0.777 mmol) in toluene (15 mL) was heated at reflux for 1 h. After cooling and leaving to stand at room temperature for 1 d, the dark-purple precipitate was filtered off, washed twice with toluene (5 mL) and dried in vacuo to give **1f**, yield 0.26 g (89 %). IR: $\tilde{\nu}$ = 1686 (CO, s), 1564 (CO, s) cm^{-1}. MS (EI, +): *m/z* (%) = 442 (66) [$C_{20}H_{22}FeN_2O_6$]$^+$, 180 (100) [$C_{12}H_8N_2$]$^+$. $C_{32}H_{30}FeN_4O_6$·1.25toluene (737.64): calcd. C 66.35, H 5.47, N 7.60; found C 66.20, H 5.58, N 7.50.

μ-(bpey)-[FeL1(EtOH)]$_2$ (1g): Black crystals of **1g** were obtained by slow diffusion in a home-made Schlenk apparatus containing [FeL1(MeOH)$_2$] (0.1 g, 0.198 mmol) and bpey (0.071 g, 0.395 mmol) in ethanol solution for 1 month.

Single-Crystal X-ray Diffraction: The X-ray crystal analysis of **1e** and **1g** was performed with a Stoe StadiVari diffractometer using graphite-monochromated Mo-K_α radiation. The X-ray analysis of bpey was performed with a Stoe IPDS II diffractometer using graphite-monochromated Mo-K_α radiation. The data were corrected for Lorentzian and polarization effects. The structures were solved by direct methods (SIR-97)[28] and refined by full-matrix least-squares techniques against $F_o^2 - F_c^2$ (SHELXL-97).[29] All hydrogen atoms were calculated in idealised positions with fixed displacement parameters. ORTEP-III[30] was used for the structure representations, SCHAKAL-99[31] to illustrate molecular packing.

CCDC 1426886 (for bpey), 1426887 (for **1e**), and 1426888 (for **1g**) contain the supplementary crystallographic data for this paper. These data can be obtained free of charge from The Cambridge Crystallographic Data Centre.

X-ray Powder Diffraction: Powder diffractograms were recorded with a STOE StadiP Powder Diffractometer (STOE, Darmstadt) using Cu-K_{α}1 radiation with a Ge Monochromator and a Mythen 1K Stripdetector in transmission geometry.

Magnetic Measurements: Magnetic measurements were carried out by using a SQUID MPMS-XL5 instrument from Quantum Design at an applied field of 5000 G and in the temperature range of 400–50 K in settle mode. The sample was prepared in a gelatine capsule held in a plastic straw. The raw data were corrected for the diamagnetic part of the sample holder and the diamagnetism of the organic ligand by using tabulated Pascal's constants.[32]

Mössbauer Spectrometry: ^{57}Fe Mössbauer spectra were recorded in transmission geometry at a constant acceleration using a conventional Mössbauer spectrometer with a 50 mCi ^{57}Co(Rh) source. The spectra were fitted by using the Recoil 1.05 Mössbauer Analysis Software.[33] The isomer shift values are given with respect to an α-Fe reference at room temperature.

Acknowledgments

Financial support from the German Science Foundation (DFG) (SFB840; project A10) and the University of Bayreuth, Germany is acknowledged. The EU-COST Network (CM1305) on spin-state reactivity is acknowledged for support.

Keywords: Spin crossover · Coordination compounds · Polymers · Solvent effects · Iron

[1] a) E. Coronado, M. Giménez-Marqués, G. Mínguez Espallargas, F. Rey, I. J. Vitórica-Yrezábal, *J. Am. Chem. Soc.* **2013**, *135*, 15986–15989; b) E. Coronado, G. Mínguez Espallargas, *Chem. Soc. Rev.* **2013**, *42*, 1525; c) G. J. Halder, *Science* **2002**, *298*, 1762–1765; d) O. Sato, J. Tao, Y.-Z. Zhang, *Angew. Chem. Int. Ed.* **2007**, *46*, 2152–2187; *Angew. Chem.* **2007**, *119*, 2200; e) J. A. Real, E. Andres, M. C. Muñoz, M. Julve, T. Granier, A. Bousseksou, F. Varret, *Science* **1995**, *268*, 265–267.

[2] P. D. Southon, L. Liu, E. A. Fellows, D. J. Price, G. J. Halder, K. W. Chapman, B. Moubaraki, K. S. Murray, J.-F. Létard, C. J. Kepert, *J. Am. Chem. Soc.* **2009**, *131*, 10998–11009.

[3] a) M. A. Halcrow (Ed.), *Spin-Crossover Materials*, Wiley, Chichester, UK, **2013**; b) P. Gütlich, H. Goodwin (Eds.), *Spin Crossover in Transition Metal Compounds I-III*, Springer, Berlin/Heidelberg, Germany, **2004**; c) M. C. Muñoz, J. A. Real, in: *Spin-Crossover Materials* (Ed.: M. A. Halcrow), Wiley, Chichester, UK, **2013**, p. 121–146; d) P. Gütlich, A. B. Gaspar, Y. Garcia, *Beilstein J. Org. Chem.* **2013**, *9*, 342–391; e) O. Roubeau, *Chem. Eur. J.* **2012**, *18*, 15230–15244; f) A. Bousseksou, G. Molnar, L. Salmon, W. Nicolazzi, *Chem. Soc. Rev.* **2011**, *40*, 3313–3335; g) I. Boldog, A. B. Gaspar, V. Martínez, P. Pardo-Ibañez, V. Ksenofontov, A. Bhattacharjee, P. Gütlich, J. A. Real, *Angew. Chem. Int. Ed.* **2008**, *47*, 6433–6437; *Angew. Chem.* **2008**, *120*, 6533; h) P. Stock, T. Pędziński, N. Spintig, A. Grohmann, G. Hörner, *Chem. Eur. J.* **2013**, *19*, 839–842; i) S. Heider, H. Petzold, G. Chastanet, S. Schlamp, T. Rüffer, B. Weber, J.-F. Létard, *Dalton Trans.* **2013**, *42*, 8575–8584; j) M. Milek, F. W. Heinemann, M. M. Khusniyarov, *Inorg. Chem.* **2013**, *52*, 11585–11592.

[4] M. C. Muñoz, J. A. Real, *Coord. Chem. Rev.* **2011**, *255*, 2068–2093.

[5] a) S. M. Neville, G. J. Halder, K. W. Chapman, M. B. Duriska, P. D. Southon, J. D. Cashion, J.-F. Létard, B. Moubaraki, K. S. Murray, C. J. Kepert, *J. Am. Chem. Soc.* **2008**, *130*, 2869–2876; b) M. Ohba, K. Yoneda, G. Agustí, M. C. Muñoz, A. B. Gaspar, J. A. Real, M. Yamasaki, H. Ando, Y. Nakao, S. Sakaki, S. Kitagawa, *Angew. Chem. Int. Ed.* **2009**, *48*, 4767–4771; *Angew. Chem.* **2009**, *121*, 4861.

[6] a) J. Linares, E. Codjovi, Y. Garcia, *Sensors* **2012**, *12*, 4479–4492; b) P. N. Martinho, T. Lemma, B. Gildea, G. Picardi, H. Müller-Bunz, R. J. Forster, T. E. Keyes, G. Redmond, G. G. Morgan, *Angew. Chem. Int. Ed.* **2012**, *51*, 11995–11999; *Angew. Chem.* **2012**, *124*, 12161; c) A. Gaspar, M. Seredyuk, P. Gütlich, *J. Mol. Struct.* **2009**, *924–926*, 9–19; d) M. Cavallini, I. Bergenti, S. Milita, G. Ruani, I. Salitros, Z.-R. Qu, R. Chandrasekar, M. Ruben, *Angew. Chem.* **2008**, *120*, 8724–8728.

[7] For recent examples, see: a) T. M. Ross, B. Moubaraki, D. R. Turner, G. J. Halder, G. Chastanet, S. M. Neville, J. D. Cashion, J.-F. Létard, S. R. Batten, K. S. Murray, *Eur. J. Inorg. Chem.* **2011**, 1395–1417; b) M. Steinert, B. Schneider, S. Dechert, S. Demeshko, F. Meyer, *Angew. Chem. Int. Ed.* **2014**, *53*, 6135–6139; *Angew. Chem.* **2014**, *126*, 6249; c) Y.-T. Wang, S.-T. Li, S.-Q. Wu, A.-L. Cui, D.-Z. Shen, H.-Z. Kou, *J. Am. Chem. Soc.* **2013**, *135*, 5942–5945; d) J. S. Costa, S. Rodríguez-Jiménez, G. A. Craig, B. Barth, C. M. Beavers, S. J. Teat, G. Aromí, *J. Am. Chem. Soc.* **2014**, *136*, 3869–3874; e) W. Vreugdenhil, J. H. Van Diemen, R. A. G. De Graaff, J. G. Haasnoot, J. Reedijk, A. M. Van Der Kraan, O. Kahn, J. Zarembowitch, *Polyhedron* **1990**, *9*, 2971–2979; f) S. Kanegawa, S. Kang, O. Sato, *Eur. J. Inorg. Chem.* **2013**, 725–729; g) M. B. Bushuev, V. A. Daletsky, D. P. Pishchur, Y. V. Gatilov, I. V. Korolkov, E. B. Nikolaenkova, V. P. Krivopalov, *Dalton Trans.* **2014**, *43*, 3906–3910.

[8] B. Weber, W. Bauer, T. Pfaffeneder, M. M. Dîrtu, A. D. Naik, A. Rotaru, Y. Garcia, *Eur. J. Inorg. Chem.* **2011**, 3193–3206.

[9] T. M. Pfaffeneder, S. Thallmair, W. Bauer, B. Weber, *New J. Chem.* **2011**, *35*, 691–700.

[10] W. Bauer, W. Scherer, S. Altmannshofer, B. Weber, *Eur. J. Inorg. Chem.* **2011**, 2803–2818.

[11] W. Bauer, T. Pfaffeneder, K. Achterhold, B. Weber, *Eur. J. Inorg. Chem.* **2011**, 3183–3192.

[12] W. Bauer, S. Schlamp, B. Weber, *Chem. Commun.* **2012**, *48*, 10222.

[13] W. Bauer, M. M. Dîrtu, Y. Garcia, B. Weber, *CrystEngComm* **2012**, *14*, 1223.

[14] R. Nowak, W. Bauer, T. Ossiander, B. Weber, *Eur. J. Inorg. Chem.* **2013**, 975–983.

[15] C. Lochenie, W. Bauer, A. P. Railliet, S. Schlamp, Y. Garcia, B. Weber, *Inorg. Chem.* **2014**, *53*, 11563–11572.

[16] W. Bauer, C. Lochenie, B. Weber, *Dalton Trans.* **2014**, *43*, 1990–1999.

[17] B. Weber, *Coord. Chem. Rev.* **2009**, *253*, 2432–2449.

[18] H. J. Shepherd, C. Bartual-Murgui, G. Molnár, J. A. Real, M. C. Muñoz, L. Salmon, A. Bousseksou, *New J. Chem.* **2011**, *35*, 1205.

[19] C. Bartual-Murgui, L. Salmon, A. Akou, N. A. Ortega-Villar, H. J. Shepherd, M. C. Muñoz, G. Molnár, J. A. Real, A. Bousseksou, *Chem. Eur. J.* **2012**, *18*, 507–516.

[20] a) D. Chiruta, C.-M. Jureschi, J. Linares, Y. Garcia, A. Rotaru, *J. Appl. Phys.* **2014**, *115*, 053523; b) M. M. Dîrtu, C. Neuhausen, A. D. Naik, A. Rotaru, L. Spinu, Y. Garcia, *Inorg. Chem.* **2010**, *49*, 5723–5736.

[21] M. Tanner, A. Ludi, *Chimica* **1980**, *34*, 23–24.

[22] E.-G. Jäger, E. Häussler, M. Rudolph, A. Schneider, *Z. Anorg. Allg. Chem.* **1985**, *525*, 67–85.

[23] a) S. Schlamp, P. Thoma, B. Weber, *Chem. Eur. J.* **2014**, *20*, 6462–6473; b) S. Schlamp, K. Dankhoff, B. Weber, *New J. Chem.* **2014**, *38*, 1965–1972.

[24] B. Weber, E.-G. Jäger, *Eur. J. Inorg. Chem.* **2009**, 465–477.

[25] R. Kulmaczewski, J. Olguín, J. A. Kitchen, Feltham, L. C. Humphrey, G. N. L Jameson, J. L. Tallon, S. Brooker, *J. Am. Chem. Soc.* **2014**, *136*, 878–881.

[26] B. Weber, E. S. Kaps, C. Desplanches, J. Létard, *Eur. J. Inorg. Chem.* **2008**, 2963–2966.

[27] a) S. Schlamp, P. Thoma, B. Weber, *Eur. J. Inorg. Chem.* **2012**, 2759–2768; b) S. Schlamp, B. Weber, A. D. Naik, Y. Garcia, *Chem. Commun.* **2011**, *47*, 7152–7154.

[28] A. Altomare, M. C. Burla, M. Camalli, G. L. Cascarano, C. Giacovazzo, A. Guagliardi, A. G. G. Moliterni, G. Polidori, R. Spagna, *J. Appl. Crystallogr.* **1999**, *32*, 115–119.

[29] a) G. Sheldrick, *SHELXL-97*, University of Göttingen, Germany, **1997**; b) G. Sheldrick, *Acta Crystallogr., Sect. A* **2008**, *64*, 112–122.

[30] a) L. Farrugia, *J. Appl. Crystallogr.* **1997**, *30*, 565; b) C. K. Johnson, M. N. Burnett, *ORTEP-III*, Oak-Ridge National Laboratory, Oak-Ridge, TN, **1996**.

[31] E. Keller, *Schakal-99*, University of Freiburg, Germany, **1999**.

[32] O. Kahn, *Molecular Magnetism*, VCH Publishers, New York, **1993**.

[33] K. Lagarec, D. G. Rancourt, *Recoil*, *Mössbauer Spectral Analysis Software for Windows 1.0*, Department of Physics, University of Ottawa, Canada, **1998**.

Received: October 15, 2015
Published Online: January 15, 2016